

## Non-Kolmogorov cascade of helicity-driven turbulence

Mouloud Kessar,<sup>1</sup> Franck Plunian,<sup>2,\*</sup> Rodion Stepanov,<sup>3,4</sup> and Guillaume Balarac<sup>1</sup>

<sup>1</sup>*Université Grenoble Alpes, CNRS, LEGI, Grenoble, France*

<sup>2</sup>*Université Grenoble Alpes, CNRS, ISTerre, Grenoble, France*

<sup>3</sup>*Institute of Continuous Media Mechanics, Korolyov str. 1, 614013 Perm, Russia*

<sup>4</sup>*Perm National Research Polytechnic University, Komsomolskii av. 29, 614990 Perm, Russia*

(Received 8 April 2015; revised manuscript received 7 September 2015; published 28 September 2015)

We solve the Navier-Stokes equations with two simultaneous forcings. One forcing is applied at a given large scale and it injects energy. The other forcing is applied at all scales belonging to the inertial range and it injects helicity. In this way we can vary the degree of turbulence helicity from nonhelical to maximally helical. We find that increasing the rate of helicity injection does not change the energy flux. On the other hand, the level of total energy is strongly increased and the energy spectrum gets steeper. The energy spectrum spans from a Kolmogorov scaling law  $k^{-5/3}$  for a nonhelical turbulence, to a non-Kolmogorov scaling law  $k^{-7/3}$  for a maximally helical turbulence. In the latter case we find that the characteristic time of the turbulence is not the turnover time but a time based on the helicity injection rate. We also analyze the results in terms of helical modes decomposition. For a maximally helical turbulence one type of helical mode is found to be much more energetic than the other one, by several orders of magnitude. The energy cascade of the most energetic type of helical mode results from the sum of two fluxes. One flux is negative and can be understood in terms of a decimated model. This negative flux, however, is not sufficient to lead an inverse energy cascade. Indeed, the other flux involving the least energetic type of helical mode is positive and the largest. The least energetic type of helical mode is then essential and cannot be neglected.

DOI: [10.1103/PhysRevE.92.031004](https://doi.org/10.1103/PhysRevE.92.031004)

PACS number(s): 47.27.Ak, 47.27.Gs

Considering the case of three-dimensional homogeneous and isotropic turbulence, Kolmogorov [1] assumed the existence of a range of scales, the so-called inertial range, in which the viscous dissipation can be neglected. In absence of dissipation the kinetic energy is a conserved quantity. In spectral space the flux of kinetic energy is constant, leading to an energy cascade from large to small scales, provided energy is injected at large scale. From a straightforward dimensional analysis the spectral density of kinetic energy  $E(k)$  can be expressed in terms of the energy injection rate  $\varepsilon$  and wave number  $k$ ,

$$E(k) \propto \varepsilon^{2/3} k^{-5/3}. \quad (1)$$

In absence of viscosity not only energy is a conserved quantity but also helicity [2,3], which is defined as

$$H(t) = \int_V \mathbf{u}(\mathbf{x}, t) \cdot \nabla \times \mathbf{u}(\mathbf{x}, t) dV, \quad (2)$$

where  $\mathbf{u}(\mathbf{x}, t)$  is the velocity field at position  $\mathbf{x}$  and time  $t$ , and integration is made over the volume  $V$ . Similarly to energy, the helicity conservation is equivalent having a constant helicity flux. Provided energy and helicity are both injected at large scale, helicity is expected to cascade jointly with energy in the inertial range, obeying the following scaling law [4–6]:

$$H(k) \propto \eta \varepsilon^{-1/3} k^{-5/3}, \quad (3)$$

where  $H(k)$  is the spectral density of helicity and  $\eta$  the injection rate of helicity. Contrary to enstrophy in two-dimensional turbulence, helicity is not sign defined and therefore not reputed for having any influence on the energy spectrum, letting the scaling law (1) remain unchanged [7].

Though the simultaneous scaling laws (1) and (3) are characteristic of the so-called helical turbulence [6], they cannot be justified from dimensional grounds like Kolmogorov did for the nonhelical turbulence. Indeed, the problem now consists in five variables  $E(k)$ ,  $H(k)$ ,  $k$ ,  $\varepsilon$ , and  $\eta$  and only two dimensions, length and time. Applying the  $\Pi$  theorem [8] and assuming that  $E(k)$  and  $H(k)$  obey some scaling laws, we find [9,10]

$$E(k) \propto \varepsilon^{7/3-a} \eta^{a-5/3} k^{-a}, \quad H(k) \propto \varepsilon^{4/3-b} \eta^{b-2/3} k^{-b}, \quad (4)$$

where  $a$  and  $b$  are two free parameters. Therefore we need additional constraints to derive the power laws for  $E(k)$  and  $H(k)$ .

One way to argue for the simultaneous  $k^{-5/3}$  scaling laws (1) and (3) is to assume that the fluxes of energy and helicity  $\Pi_E(k)$  and  $\Pi_H(k)$  are constant in the inertial range, such that  $\Pi_E(k) = \varepsilon$  and  $\Pi_H(k) = \eta$ . In addition, we have to set that the characteristic times  $\tau_E$  and  $\tau_H$  for the energy and helicity transfers are given by the turbulence turnover time  $\tau_E = \tau_H \propto (\varepsilon k^2)^{-1/3}$ . Then estimating both energy and helicity fluxes as [5,11]

$$\Pi_E(k) = kE(k)/\tau_E(k), \quad \Pi_H(k) = kH(k)/\tau_H(k), \quad (5)$$

leads to (1) and (3). In the notations of (4) this would correspond to  $a = b \equiv 5/3$ .

Instead we could think of spectral laws independent of  $\varepsilon$ , leading to [5]

$$E(k) \propto \eta^{2/3} k^{-7/3}, \quad H(k) \propto \eta^{2/3} k^{-4/3}. \quad (6)$$

In the notations of (4) this would correspond to  $a = b + 1 \equiv 7/3$ . Providing evidence of such scaling laws (6), is still a challenging issue and has never been observed so far in direct numerical simulations. Recently, a step forward has been made by solving the so-called decimated Navier-Stokes (NS)

\*Franck.Plunian@ujf-grenoble.fr

equations [12,13]. It consists in splitting each Fourier mode of the velocity field in positive and negative helical modes, and in solving the NS equations keeping only one type of mode. By construction the resulting turbulence is then exactly maximally helical, i.e.,  $|H(k)| = kE(k)$ . In such a decimated model helicity is still a conserved quantity, but now it gets the property to be sign definite. It then plays a role similar to enstrophy in 2D turbulence, leading to a  $k^{-5/3}$  inverse cascade of energy at scales larger than the forcing scale [12]. In the inertial range the helicity cascade is direct, with an energy scaling law  $E(k) \propto k^{-7/3}$  [13]. In a recent experimental study [14] two scaling laws have also been found, the authors arguing for the existence of two such opposite cascades, but with dominant nonlocal transfers leading to  $E(k) \propto k^{-1}$  and  $E(k) \propto k^{-2}$ .

Here we present another strategy that does not assume any simplification of the NS equations and which is based on the fact that the scaling laws (6) do not depend on  $\varepsilon$ . Such a  $\varepsilon$  independence is expected as soon as  $\tau_H \leq \tau_E$ , then speaking of a helicity-driven turbulence. From (5) and applying the exact constraint  $|H(k)| \leq kE(k)$ , a sufficient condition for having  $\tau_H \leq \tau_E$  is given by

$$\Pi_H(k) \geq k\Pi_E(k). \quad (7)$$

One way to satisfy such a flux condition (7) is to inject energy at large scale such that  $\Pi_E(k) = \varepsilon$  and helicity at all scales such that  $\Pi_H(k) \geq k\varepsilon$ . This is the strategy that is followed in the present Rapid Communication using direct numerical simulation of the NS equations. A similar strategy has been used in [15,16] using a helical shell model.

Using a pseudospectral code we solve the NS equations

$$\partial_t \mathbf{u} = -(\mathbf{u} \cdot \nabla) \mathbf{u} - \nabla p + \nu \nabla^2 \mathbf{u} + \mathbf{f}, \quad (8)$$

where  $\nu$ ,  $p$ , and  $\mathbf{f}$  are, respectively, the viscosity, the pressure, and the flow forcing. The forcing is divided into two parts  $\mathbf{f} = \mathbf{f}^E + \mathbf{f}^H$ , where  $\mathbf{f}^E$  is the energy forcing applied at some given large scale  $k_F^{-1}$ , and  $\mathbf{f}^H$  is the helicity forcing applied at all scales within the inertial range.

Both parts of the forcing  $\mathbf{f}^E$  and  $\mathbf{f}^H$  are delta correlated in time and divergence-free. Following [17] they are defined such that the power input comes from the force-force correlation only and not from the velocity-force correlation. In spectral space this corresponds to

$$\mathbf{u}_k^* \cdot \mathbf{f}_k^E + \text{c.c.} = 0, \quad (9)$$

$$\mathbf{u}_k^* \cdot \mathbf{f}_k^H + \text{c.c.} = 0, \quad (10)$$

where  $\mathbf{f}_k^E$  and  $\mathbf{f}_k^H$  are the Fourier coefficients of  $\mathbf{f}^E$  and  $\mathbf{f}^H$ .

For  $\mathbf{f}^E$  we use the exact same forcing as in [17] with a force-force correlation given by

$$|\mathbf{f}_k^E|^2 = F(\mathbf{k})/2\pi k^2, \quad (11)$$

where  $F(\mathbf{k})$  obeys to a Gaussian distribution around  $k = k_F$ . As in [17]  $F(\mathbf{k})$  is defined as inversely proportional to the time step of the computation, in order to guarantee an injection rate of energy which is independent from the value of the time step. The level of helicity injected by  $\mathbf{f}^E$  is not controlled *a priori*, but the results show that it is statistically insignificant.

In order to inject helicity the forcing  $\mathbf{f}^H$  has to satisfy, in spectral space,

$$(\nabla \times \mathbf{u})_k^* \cdot \mathbf{f}_k^H + \mathbf{u}_k^* \cdot (\nabla \times \mathbf{f}^H)_k + \text{c.c.} = \eta(\mathbf{k}), \quad (12)$$

where  $\eta(\mathbf{k})$  is a helicity injection rate per unit volume. We take

$$\eta(\mathbf{k}) = 0 \text{ for } |\mathbf{k}| < k_F, \quad (13)$$

$$\eta(\mathbf{k}) = \eta_0(|\mathbf{k}|/k_F)^{-\alpha} \text{ for } |\mathbf{k}| \geq k_F \quad (14)$$

with  $\alpha = 2.2$  in order to have a spectral density of helicity injection rate  $|\mathbf{k}|^2 \eta(\mathbf{k})$  almost flat. Of course, such a forcing extending on the whole inertial range might change the intermittency properties of the turbulence [18]. However, we find that the level of dissipation with and without  $\mathbf{f}^H$  is statistically unchanged. Finally, two issues have to be clarified, both related to the fact that the energy power coming from the force-force correlation of  $\mathbf{f}^H$  is not controlled *a priori* and that we need to keep it at a level sufficiently lower than the one injected by  $\mathbf{f}^E$ . These rather technical issues are detailed in the Appendix.

Applying a classic criterion [19] in order to ensure the resolution of a sufficiently large range of dissipation scales, taking a grid of  $256^3$  points and setting  $\nu = 2 \cdot 10^{-3}$  and  $R_\lambda = 100$ , where  $R_\lambda$  is the Reynolds number based on the Taylor microscale, leads to an energy injection rate  $\varepsilon \approx 0.2$  and a forcing wave number  $k_F \approx 2.2$ . Finally, all subsequent results correspond to statistically steady states.

In Fig. 1 top and bottom, the spectral density of energy  $E(k)$  and relative helicity  $H(k)/[kE(k)]$  are represented for five values of helicity injection  $\eta_0$ , ranging from nonhelical turbulence ( $\eta_0 = 0$ ) to maximally helical turbulence ( $\eta_0 = 5$ ). Clearly, increasing  $\eta_0$  steepens the energy spectral density at large scales, with a scaling law varying from  $k^{-5/3}$  for nonhelical, to  $k^{-7/3}$  for maximally helical turbulence (top of Fig. 1). For  $\eta_0 \neq 0$  a well defined spectrum of relative helicity is obtained with a rather flat part. For  $\eta_0 = 1$  and  $\eta_0 = 5$  the relative helicity is about unity over an extended range of scales, showing that the turbulence is close to a maximally helical state (bottom of Fig. 1).

The fluxes of energy and helicity,  $\Pi_E(k)$  and  $\Pi_H(k)$ , are plotted in the top and bottom of Fig. 2, for again the same five values of  $\eta_0$ . In the top figure we see that  $\Pi_E(k)$  is almost independent of  $\eta_0$ , showing that the spurious energy injection produced by the helical forcing  $\mathbf{f}^H$  is small compared to the energy injected by  $\mathbf{f}^E$ . On the other hand, in the bottom figure we see that  $\Pi_H(k)$  is getting higher when increasing the value of  $\eta_0$ . Therefore we conclude *a posteriori* that the injections of energy and helicity are well prescribed by  $\mathbf{f}^E$  and  $\mathbf{f}^H$ , respectively.

Relying on (5) and knowing the flux and spectral density of energy and helicity, we can calculate the two characteristic times,  $\tau_E(k)$  and  $\tau_H(k)$ , in order to determine which one is the smallest and therefore which one controls the turbulence. In Fig. 3 the ratio  $\tau_H(k)/\tau_E(k)$  is plotted for  $\eta_0 = 0.05, 0.3, 1$ , and  $5$ . For sufficiently large values of  $\eta_0$ , typically  $\eta_0 = 1$  and  $\eta_0 = 5$ , we see that for  $k \in [3, 12]$   $\tau_H(k)/\tau_E(k) < 1$ , suggesting a turbulence governed by the helicity injection

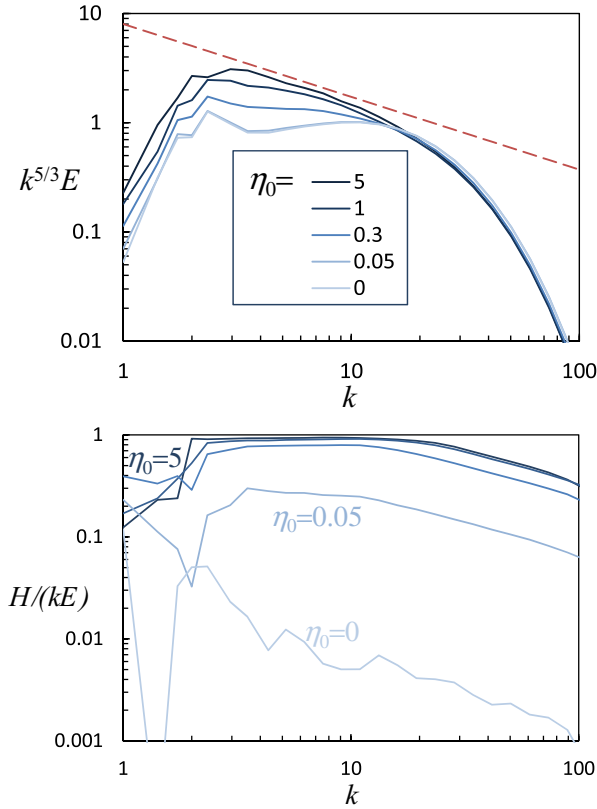


FIG. 1. (Color online) Spectral density of energy (top) and relative helicity (bottom), for five values of the helicity injection rate:  $\eta_0 = 0, 0.05, 0.3, 1$ , and  $5$ . In the top figure the energy is normalized by  $k^{-5/3}$  and the red dashed curve corresponds to  $k^{-7/3}$ .

rate. On the other hand, for low values of  $\eta_0$ , typically  $\eta_0 = 0.05$  and  $\eta_0 = 0.3$ , and in the same range of scales we find  $\tau_H(k)/\tau_E(k) > 1$ , suggesting a turbulence governed by the energy injection.

Up to now it has been demonstrated that injecting a sufficiently high rate of helicity over the whole inertial range of a turbulent flow leads to a  $k^{-7/3}$  scaling law for the energy spectral density and that the characteristic time of such maximally helical turbulence is the one based on the helicity injection rate.

Now the question arises how our results fit in with the scenario described by the decimated model [12,13]. As the injection of positive helicity is made at all scales and at each time step, we expect a strong dominance of the positive helical modes compared to the negative helical modes. Then according to [12,13] we could expect an inverse cascade of energy. However, the energy fluxes plotted in Fig. 2 are always positive, demonstrating a direct cascade of energy. To clarify this paradox we now analyze our results in terms of helical modes decomposition.

In Fourier space the velocity field is split into two helical modes per wave vector

$$\mathbf{u}(\mathbf{k}) = \mathbf{u}^+(\mathbf{k}) + \mathbf{u}^-(\mathbf{k}) \quad (15)$$

$$= u^+(\mathbf{k})\mathbf{h}^+(\mathbf{k}) + u^-(\mathbf{k})\mathbf{h}^-(\mathbf{k}), \quad (16)$$

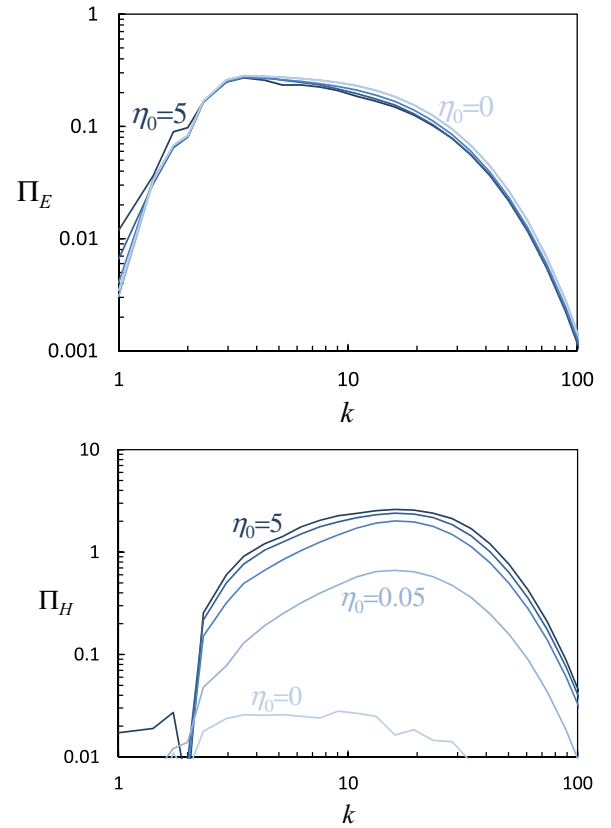


FIG. 2. (Color online) Flux of energy  $\Pi_E$  (top) and helicity  $\Pi_H$  (bottom) for the same five values of  $\eta_0$  as in Fig. 1 and same color code.

where  $u^\pm$  are complex scalars and  $\mathbf{h}^\pm$  are the eigenvectors of the curl operator satisfying  $\mathbf{ik} \times \mathbf{h}^\pm = \pm|\mathbf{k}|\mathbf{h}^\pm$  [20,21]. The energy spectral density of each helical mode, defined by  $E^\pm(k) = |u^\pm(k)|^2$ , is plotted in Fig. 4, for again the same five values of  $\eta_0$  as in Fig. 1. For each value of  $\eta_0$  we observe that both spectra  $E^\pm(k)$  obey to the same scaling laws, again varying from  $k^{-5/3}$  for  $\eta_0 = 0$  to  $k^{-7/3}$  for  $\eta_0 = 5$ . This is consistent with the results of Fig. 1 and the relation  $E(k) = E^+(k) + E^-(k)$ . For  $\eta_0 = 0$  both spectra  $E^\pm(k)$  are identical as expected for a nonhelical turbulence. Increasing  $\eta_0$

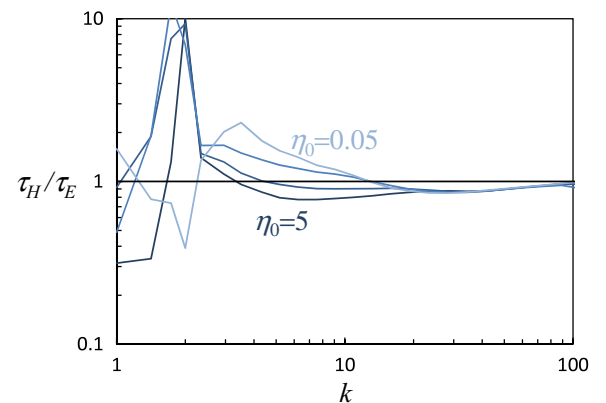


FIG. 3. (Color online) Ratio  $\tau_H(k)/\tau_E(k)$  versus  $k$  for  $\eta_0 = 0.05, 0.3, 1$ , and  $5$  and same color code as in Fig. 1.

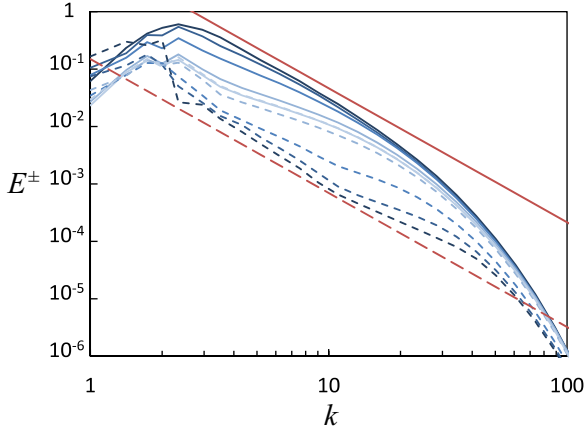


FIG. 4. (Color online) Energy spectra  $E^+(k)$  (solid line) and  $E^-(k)$  (dashed line) for the same five values of  $\eta_0$  as in Fig. 1 and the same color code. Increasing  $\eta_0$  the curves spread from the center towards the two (red) dashed and solid straight lines corresponding to  $k^{-7/3}$ .

both spectra separate apart from each other,  $E^+(k)$  prevailing over  $E^-(k)$  by two orders of magnitude for  $\eta_0 = 5$ .

Following [22,23] we now analyze the fluxes between the helical modes. We denote by  $\Pi_b^{a<}(k)$  the energy flux from the inside region of a  $\mathbf{u}^a$  sphere of radius  $k$  to all wave numbers of  $\mathbf{u}^b$ , where  $a, b \equiv \pm$ . It is defined as

$$\Pi_b^{a<}(k) = \int_{|\mathbf{k}'| \leq k} \mathbf{u}^a(\mathbf{k}') \cdot \mathcal{F}\{(\mathbf{u} \cdot \nabla)\mathbf{u}^b\}(\mathbf{k}') d\mathbf{k}', \quad (17)$$

where  $\mathcal{F}\{(\mathbf{u} \cdot \nabla)\mathbf{u}^b\}$  denotes the Fourier transform of the non linear term  $(\mathbf{u} \cdot \nabla)\mathbf{u}^b$ . The four fluxes  $\Pi_{\pm}^{\pm<}(k)$  are represented schematically in Fig. 5 (top). They are plotted in Fig. 5 (bottom) for  $\eta_0 = 0$  (light curves) and  $\eta_0 = 5$  (dark curves). The sum of these four fluxes corresponds to the energy flux plotted in Fig. 2 (top). For  $\eta_0 = 5$  the fluxes (c)  $\Pi_{-}^{+<}(k)$  and (d)  $\Pi_{+}^{-<}(k)$  are much larger than for  $\eta_0 = 0$ . In addition, they are of opposite sign corresponding to a net flux of energy from the positive to the negative helical modes, balancing each other at small scales (large  $k$ ).

Let us now focus on the flux (a)  $\Pi_{+}^{+<}(k)$ . By definition the energy flux from the inside region of a  $\mathbf{u}^+$  sphere of radius  $k$  to itself is zero. This implies that  $\Pi_{+}^{+<}(k) = \Pi_{+>}^{+<}(k)$ , which is the energy flux from the inside region of the  $\mathbf{u}^+$  sphere of radius  $k$  to the outside of that same  $\mathbf{u}^+$  sphere. Now the fact that in Fig. 5 (bottom)  $\Pi_{+>}^{+<}(k)$  is always positive means that there is a direct cascade of energy. This is in contrast with the inverse cascade found with the decimated model of [12,13].

Finally, we push one step further by splitting the flux  $\Pi_{+>}^{+<}(k)$  into two parts  $\Pi_{+>}^{+<}(k) = {}^+\Pi_{+>}^{+<}(k) + {}^-\Pi_{+>}^{+<}(k)$  with

$${}^{\pm}\Pi_{+>}^{+<}(k) = \int_{|\mathbf{k}'| \leq k} \mathbf{u}^{\pm}(\mathbf{k}') \cdot \mathcal{F}\{(\mathbf{u}^{\pm} \cdot \nabla)\mathbf{u}^+\}(\mathbf{k}') d\mathbf{k}'. \quad (18)$$

In (18)  ${}^{\pm}\Pi_{+>}^{+<}(k)$  denotes the energy flux from the inside region of a  $\mathbf{u}^+$  sphere of radius  $k$  to the outside of the  $\mathbf{u}^+$  sphere, with  $\mathbf{u}^{\pm}$  acting as a mediator on the nonlinear interactions. Both fluxes  ${}^{\pm}\Pi_{+>}^{+<}(k)$  are plotted in Fig. 6 for again the same five values of  $\eta_0$  as in Fig. 1. The flux  ${}^+\Pi_{+>}^{+<}(k)$  is always negative in agreement with the arguments given in [12,13] for

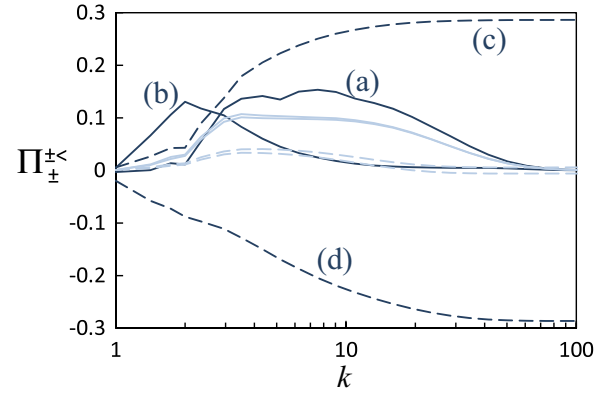
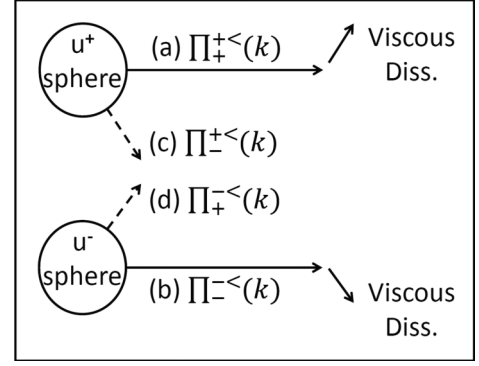


FIG. 5. (Color online) Top: Various energy fluxes in helical turbulence.  $\Pi_b^{a<}(k)$  denotes the energy flux from the inside region of a  $\mathbf{u}^a$  sphere of radius  $k$  to all wave numbers of  $\mathbf{u}^b$ , where  $a, b \equiv \pm$ . Bottom: The dark (light) curves correspond to  $\eta_0 = 5$  ( $\eta_0 = 0$ ). The solid curves correspond to  $\Pi_{+>}^{+<}(k)$  and  $\Pi_{+>}^{-<}(k)$ , and the dashed curves to  $\Pi_{->}^{+<}(k)$  and  $\Pi_{->}^{-<}(k)$ . For  $\eta_0 = 5$ , (a) corresponds to  $\Pi_{+>}^{+<}(k)$ , (b) to  $\Pi_{+>}^{-<}(k)$ , (c) to  $\Pi_{->}^{+<}(k)$ , and (d) to  $\Pi_{->}^{-<}(k)$ .

the decimated model. However, the flux  ${}^-\Pi_{+>}^{+<}(k)$  is positive and always the largest in absolute value. This shows that even if the turbulence is strongly positively helical, the presence of negative helical modes is nevertheless essential to give

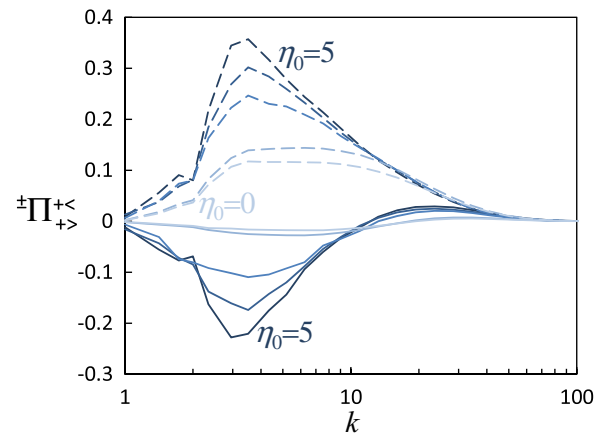


FIG. 6. (Color online) Energy fluxes  ${}^+\Pi_{+>}^{+<}(k)$  (solid) and  ${}^-\Pi_{+>}^{+<}(k)$  (dashed) for the same five values of  $\eta_0$  as in Fig. 1 and same color code. Increasing  $\eta_0$  from 0 to 5 the solid curves at  $k = 3$  decrease and the dashed curves increase.

the right sign of the energy fluxes. Though the decimated model is mathematically appealing because it reproduces an exact maximally helical flow, it is eventually singular as in practice the existence of both types of helical modes cannot be avoided. This result also supports the choice made in helical shell models [23] in which two helical modes can interact only if they have opposite helicities.

ISterre and LEGI are part of Labex OSUG@2020 (Grant No. ANR10LABX56) and Labex Tec21 (Grant No. ANR11LABX30). We acknowledge support from region Rhône-Alpes through the CIBLE program, IDRIS and CIMENT for HPC resources. We acknowledge provision for computational resources of the URAN and TRITON clusters of Russian Academy of Science, Ural Branch.

#### APPENDIX: THE HELICITY FORCING

The helicity forcing is defined in its spectral form as

$$\mathbf{f}_k^H = \mathbf{k} \times \mathbf{p}(\mathbf{k}, t) \quad (\text{A1})$$

with

$$\mathbf{p}(\mathbf{k}, t) = a(\mathbf{k}, t)\mathbf{e}_1(\mathbf{k}, t) + ib(\mathbf{k}, t)\mathbf{e}_2(\mathbf{k}, t), \quad (\text{A2})$$

$\mathbf{e}_1(\mathbf{k}, t)$  and  $\mathbf{e}_2(\mathbf{k}, t)$  being two unit vectors with directions changing randomly at each time step. The resolution of Eqs. (10) and (12) leads to

$$a(\mathbf{k}, t) = -\frac{\eta(\mathbf{k})}{4D|\mathbf{k}|^2}(\text{Im}(\mathbf{u}_k), \mathbf{k}, \mathbf{e}_2), \quad (\text{A3})$$

$$b(\mathbf{k}, t) = \frac{\eta(\mathbf{k})}{4D|\mathbf{k}|^2}(\text{Re}(\mathbf{u}_k), \mathbf{k}, \mathbf{e}_1), \quad (\text{A4})$$

with

$$D(\mathbf{k}, t) = (\text{Re}(\mathbf{u}_k), \mathbf{k}, \mathbf{e}_1)[\text{Re}(\mathbf{u}_k) \cdot \mathbf{e}_2] + (\text{Im}(\mathbf{u}_k), \mathbf{k}, \mathbf{e}_2)[\text{Im}(\mathbf{u}_k) \cdot \mathbf{e}_1]. \quad (\text{A5})$$

As stated above, the energy forcing  $\mathbf{f}^E$  is inversely proportional to the time step [17]. Conversely  $\mathbf{f}^H$  does not depend on the time step, implying that the level of energy rate which comes from the force-force correlation of  $\mathbf{f}^H$  is proportional to the time step. Therefore, provided the time step is sufficiently small, the energy rate coming from the force-force correlation of  $\mathbf{f}^H$  can be maintained at a sufficiently low level compared to the energy rate coming from the force-force correlation of  $\mathbf{f}^E$ . In other words, to maintain a spurious power injected by  $\mathbf{f}^H$  at a low level it is necessary to decrease the time step when increasing  $\eta_0$ .

Finally, we apply a *clipping* condition in order to prevent any spurious energy injection coming from singular solutions of Eqs. (10) and (12). Indeed, as the forcing  $\mathbf{f}^H$  is random in time we cannot prevent the value of  $D$  given in (A5) to be zero and lead to singular solutions  $a(\mathbf{k}, t)$  and  $b(\mathbf{k}, t)$ . In addition, we do not want to force energy or helicity in the dissipative range (corresponding to scales  $k \geq k_v$  where  $k_v \approx \varepsilon^{1/4} \nu^{-3/4}$ ). Therefore, at each time step the helical forcing  $\mathbf{f}^H$  is applied provided the following condition is satisfied:

$$D(\mathbf{k}, t) \geq |\mathbf{k}||\mathbf{u}_k|^2 \left[ A + B \left( \frac{k}{k_v} \right)^\beta \right], \quad (\text{A6})$$

where  $A$ ,  $B$ , and  $\beta$  are positive constants whose values depend on  $\eta_0$ .

- 
- [1] A. Kolmogorov, Dokl. Akad. Nauk. SSSR **30**, 299 (1941).  
 [2] J. Moreau, C. R. Acad. Sci. Paris **252**, 2810 (1961).  
 [3] H. Moffatt, *J. Fluid Mech.* **35**, 117 (1969).  
 [4] M. Lesieur, U. Frisch, and A. Brissaud, *Ann. Geophys.* **27**, 151 (1971).  
 [5] A. Brissaud, U. Frisch, J. Leorat, M. Lesieur, and A. Mazure, *Phys. Fluids* **16**, 1366 (1973).  
 [6] Q. Chen, S. Chen, G. L. Eyink, and D. D. Holm, *Phys. Rev. Lett.* **90**, 214503 (2003).  
 [7] P. D. Mininni, A. Alexakis, and A. Pouquet, *Phys. Rev. E* **74**, 016303 (2006).  
 [8] G. I. Barenblatt, *Dimensional Analysis* (Gordon and Breach, New York, 1987).  
 [9] E. Golbraikh and S. Moiseev, *Phys. Lett. A* **305**, 173 (2002).  
 [10] E. Golbraikh, *Phys. Lett. A* **354**, 214 (2006).  
 [11] R. H. Kraichnan, *J. Fluid Mech.* **47**, 525 (1971).  
 [12] L. Biferale, S. Musacchio, and F. Toschi, *Phys. Rev. Lett.* **108**, 164501 (2012).  
 [13] L. Biferale, S. Musacchio, and F. Toschi, *J. Fluid Mech.* **730**, 309 (2013).  
 [14] E. Herbert, F. Daviaud, B. Dubrulle, S. Nazarenko, and A. Naso, *Europhys. Lett.* **100**, 44003 (2012).  
 [15] A. Shestakov, E. Golbraikh, R. Stepanov, and P. Frick, Proceedings of the 14th European Turbulence Conference, 2013 (unpublished).  
 [16] R. Stepanov, E. Golbraikh, P. Frick, and A. Shestakov, *arXiv:1508.07236*.  
 [17] K. Alvelius, *Phys. Fluids* **11**, 1880 (1999).  
 [18] L. Biferale, A. S. Lanotte, and F. Toschi, *Phys. Rev. Lett.* **92**, 094503 (2004).  
 [19] S. B. Pope, *Turbulent Flows* (Cambridge University Press, Cambridge, 2000).  
 [20] F. Waleffe, *Phys. Fluids* **4**, 350 (1992).  
 [21] T. Lessinnes, F. Plunian, R. Stepanov, and D. Carati, *Phys. Fluids* **23**, 035108 (2011).  
 [22] M. K. Verma, *Phys. Rep.* **401**, 229 (2004).  
 [23] F. Plunian, R. Stepanov, and P. Frick, *Phys. Rep.* **523**, 1 (2013).